Journal of Alloys and Compounds 509 (2011) 1760–1767

Contents lists available at ScienceDirect

Journal of Alloys and Compounds

journal homepage: www.elsevier.com/locate/jallcom

Research on a novel force sensor based on giant magnetostrictive material and its model

Zhen-Yuan Jia, Hui-Fang Liu*, Fu-Ji Wang, Chun-Ya Ge

Key Laboratory for Precision and Non-Traditional Machining Technology of Ministry of Education, Dalian University of Technology, Dalian 116024, PR China

ARTICLE INFO

Article history:
Received 27 April 2010
Received in revised form 8 October 2010
Accepted 9 October 2010
Available online 21 October 2010

Keywords:
Magnetostrictive force sensor
Giant magnetostrictive material rod
Inverse magnetostrictive effect
Model

ABSTRACT

A novel magnetostrictive force sensor which can measure static force and dynamic force using giant magnetostrictive material rod as the sensitive element was studied. A special structure was proposed which was a stainless steel ring around the Hall sensor to improve the force measuring sensitivity. In view of the hysteresis nonlinearity of the giant magnetostrictive material and actual working process of the sensor, a model was established based on the combination of Jiles–Atherton model and magnetomechanical effect method. The unknown magnetic and magnetostrictive parameters in the model were identified by a hybrid algorithm of genetic algorithm and simulated annealing algorithm. Moreover, the numerical solution method and simulation process of the model were expounded in detail. The results showed that the force measuring sensitivity is about 6.14 times higher than that of the sensor without this special structure. The model can reveal the magnetization process mechanism clearly and describe the relationship between force input and electromagnetic output effectively.

1. Introduction

The wise words of an old engineer, "If you can't measure it, you can't control it" demonstrate the importance of sensors in system design. Sensor is the first link for measuring and automatic control [1]. In recent years, there is a new type of force sensor which is magnetostrictive force sensor. Compared with the other force sensors, it has obvious advantages, such as the efficient coupling between the elastic and magnetic states, withstanding heavy load, short response time, low power consumption, better capability to adapt to harsh working environment, etc. [2]. The principle of magnetostrictive force sensor based on the inverse magnetostrictive effect is utilizing the characteristics that under the action of external force, it generates mechanical stress in ferromagnetic materials and leads to relative permeability change [3]. It converts the force input into the electromagnetic signal output.

At present, the sensitive materials of magnetostrictive force sensors mainly are silicon steel, permalloy, iron, etc. Dalian University of Technology investigated a magnetostrictive force sensor based on permalloy [4]. Kleinke and Uras developed a contacting magnetostrictive force sensor in which SAE 1018 steel was used as the sensitive material [5]. Baudendistel and Turner studied a ring inverse-magnetostrictive force sensor [1]. However, the magnetostrictive coefficient of these materials used in these sensors were small (10^{-6}–10^{-5}) and sensitivity were poor. The emergence of giant magnetostrictive material (GMM) provides a new type of sensitive material for the development of magnetostrictive force sensor. By right of its excellent characteristics of large magnetostrictive coefficient at room temperature (1500×10^{-6}–2000×10^{-6}) which is 100–1000 times higher than that of common magnetostrictive material [6], low magnetocrystalline anisotropy, high magnetomechanical coupling coefficient, fast response speed, etc., GMM attracts wide attention at home and in abroad academic circles, and industrial community [7].

Currently, for the study of GMM, it mainly focuses on material properties and actuators based on the magnetostrictive effect which refers to the shape and length of ferromagnetic materials change under the action of an external magnetic field [8]. Moreover, they are relatively mature. Wang et al. investigated the electrical resistance load effect on magnetoelectric coupling of magnetostrictive laminated composite. They found that magnetoelectric coefficient and resonance frequency increase with the increase of electrical resistance load and the maximum magnetoelectric power occurs in open-circuit condition [9,10]. Jia et al. proposed a giant magnetostrictive microdisplacement actuator and its control system which could self-sense its output displacement and the magnetic flux density in GMM rod [11,12]. Its response

* Corresponding author at: School of Mechanical Engineering, Dalian University of Technology, No. 2, Linggong Road, Ganjingzi District, Dalian, Liaoning Province, PR China, 116024. Tel.: +86 13940925372; fax: +86 41184708812.
E-mail address: huifangl@163.com (H.-F. Liu).

0925-8388/$ – see front matter © 2010 Elsevier B.V. All rights reserved.
doi:10.1016/j.jallcom.2010.10.035

frequency and precision can reach 1 kHz and 0.16–0.41 μm respectively. Subsequently, based on the knowledge of magnetostriction generating mechanism, Jia et al. proposed a dynamic nonlinearity model which regards Terfenol-D rod as a viscoelastic rod continuous system [13]. The control model may describe the dynamic characteristics precisely and improve control precision of the microdisplacement actuator. Grunwald and Olabi made a magnetic parametrical analysis with magnetic simulation of the magnetostrictive actuator and developed a magnetostrictive actuator with a higher energy density. The blocked force of the actuator with a GMM rod of 8 mm diameter may reach 4500 N [14]. Angara et al. designed a high speed (up to >5 kHz), low power magnetostrictive mirror deflector, which meet the requirement in lidar and rapidly tunable laser systems [15]. Zhejiang University researched on magnetostrictive materials high-speed powerful solenoid valve and actuator. In addition, GMM have been practically used in the fields of high power underwater acoustic transducers, linear motors, rail diesel injection system, vibration absorber of turboprop aircraft, micro-feed device, hybrid magnetostrictive device, etc. [16,17].

However, few investigations have been done on giant magnetostrictive force sensor based on the inverse magnetostrictive effect of GMM. Yang developed a giant magnetostrictive force sensor and established its magneto-mechanical strongly coupled model [2]. Since Gauss meter was used in the sensor to measure the magnetic flux density variation in the air gap, the measuring accuracy was relatively low and measuring position was hard to control. Moreover, the sensor cannot measure dynamic force effectively. Furthermore, hysteresis is one of the most significant disadvantages in GMM. There is hysteresis nonlinearity relationship among the external force, magnetization and magnetic flux density. It limits the output performance and control precision severely. The coupled linear magnetomechanical constitutive equations are widely applied in giant magnetostrictive force and magnetic hysteresis modeling [18,19]. It is helpful to understand the working principle of sensor. However, the model does not consider the nonlinearity characteristics of material. Thus, it is only suitable for describing the working process of the sensor under low force signal. Based on the classical Preisach model, Bergqvist and Engdahl [20] established a stress-dependent magnetic Preisach hysteretic model. It had a good ability in predicting hysteretic nonlinearity. Since it was a black-box model based on experimental data, it could not reveal the process mechanism and was difficult to adapt to working condition changing. In order to realize the accurate control, an effective model must be established which can consider the hysteresis existing in the magnetization process and can describe the working process of the sensor. A reliable and versatile mathematical model will lend insight into the behavior of giant magnetostrictive force sensor and become a valuable design tool.

In this paper, a novel high sensitive giant magnetostrictive force sensor which uses GMM rod as the sensitive element was presented. It can measure static force and dynamic force simultaneously. A special structure of stainless steel ring in the sensor is proposed to improve the sensor sensitivity. Furthermore, based on the combination of Jiles–Atherton model and magnetomechanical effect approach, a model which can effectively describe the hysteresis problem was established. This paper is organized as follows. In Section 2, the measure principle and sensor structure are expounded. In Section 3, a model for the sensor is established through the combination of Jiles–Atherton model and magnetomechanical effect approach. Section 4 introduces the model parameters identification, numerical solution method and simulation results. Moreover, there is a comparison between the results of model and experiment, which verifies the model validity. In Section 5, sensitivity of the novel sensor is studied by experiment. Section 6 concludes.

2. Structure of the sensor

The main principle of the giant magnetostrictive force sensor is utilizing the inverse magnetostrictive effect occurred in GMM rod. Under a constant magnetic field, the magnetic permeability of GMM changes when it is subjected to an external force. This causes changing of magnetic flux density in GMM rod. On the one hand, the static force can be measured through measuring the variation of magnetic flux density. On the other hand, under the action of dynamic force, the magnetic flux density changes dynamically. Then, utilizing the Faraday effect, there generates induced voltage in pickup coil and the dynamic force can be measured by the induced voltage.

The giant magnetostrictive force sensor is designed modularly in the paper and its structure is shown in Fig. 1. The sensitive element of the sensor is a GMM rod which is made of TbDyFe. External force is applied to the exerting force mechanism directly. It is transferred to GMM rod through upper magnetic conductive gasket. When it is a static force, the magnetic flux density changes on the instant of applying force and then keeps invariant. The magnetic flux density in the GMM rod is measured by a Hall sensor pasted on the surface of the under magnetic conductive plate by nonmagnetic glue, and thereby the static force can be calculated. While a dynamic force applies to the sensor, the magnetic flux density changes along with the force real-timely. There is an induced voltage generated in pickup coil on the basis of Faraday effect. Consequently, the static and dynamic force inputs are converted into magnetic signal and electrical signal outputs respectively.

The giant magnetostrictive force sensor realizes static force measuring through an integrated linear Hall sensor which measures a magnetic flux density proportional to the variation of magnetic flux density in GMM rod with respect to the external force. Therefore in order to improve the force measuring sensitivity, that is enhancing the proportional coefficient between the magnetic flux density measured by Hall sensor and the actual magnetic flux density in GMM rod, a special structure around Hall sensor with a stainless steel ring is proposed in the paper. The structure is shown as the amplifying part in Fig. 1. It is designed according to the following principle: the magnetic flux like an electric current takes the way with the least resistance. If the structure around the Hall sensor were made of the flux guiding material, the magnetic resistance in this path would have been lower than a path crossing Hall sensor. Therefore, the magnetic resistance around the sensor had to be changed in such a way that there is no path for the flux having a lower resistance. The relative magnetic permeability of the stainless steel ring is near to one, so it magnetically behaves like the sensor and the surrounding air. Thus, magnetic flux can pass Hall sensor, stainless steel ring and air averagely.

Since the inverse magnetostrictive effect characteristic of GMM rod is related to bias magnetic field intensity, GMM rod must be premagnetization so as to make it in the optimal state. An excitation coil wound on the outer layer of coil frame and supplied DC current is used to generate bias magnetic field which can be adjusted real-timely. The bias magnetic field can be measured by Hall sensor before the giant magnetostrictive force sensor starting work formally. Due to its quite low permeability is about 5, GMM rod is not suitable to be used as flux guiding element in the construction of the sensor. The upper and under magnetic conductive plate, and upper and under magnetic conductive gasket made of highly permeable electrical pure iron DT4 are designed to work as the flux guidance elements and ensure that the magnetic flux density distributes uniformly in GMM rod.

The outer sleeve and mounting cover with external and internal thread respectively made of antimagnetic stainless steel material connect together through thread. They package the whole giant magnetostrictive force sensor in the internal to prevent the inter-

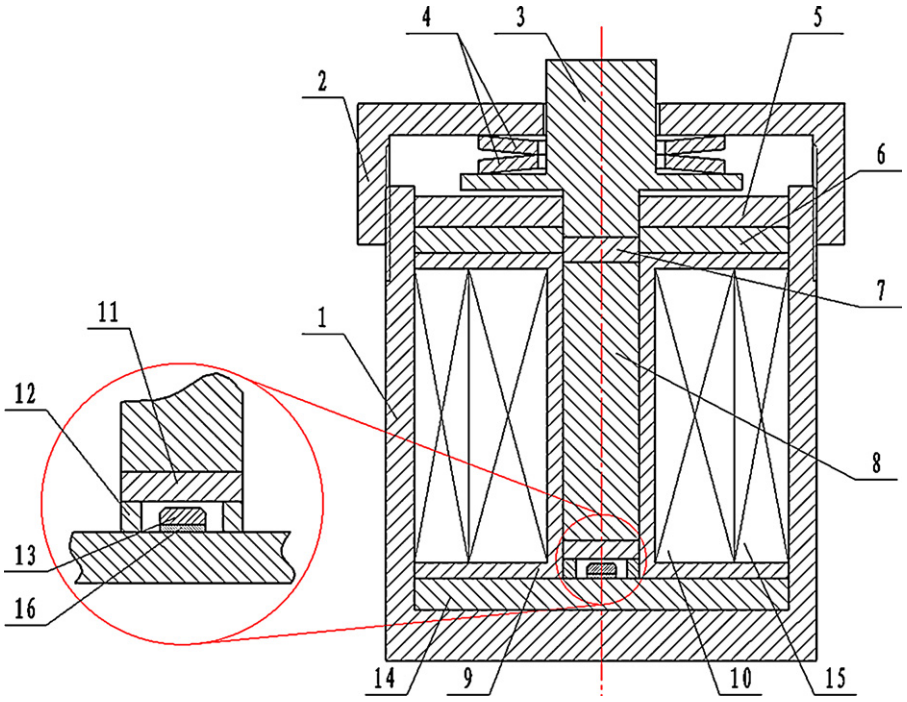

Fig. 1. Structure diagram of the giant magnetostrictive force sensor. 1: Outer sleeve, 2: mounting cover, 3: exerting force mechanism, 4: disk springs, 5: end cover, 6: upper magnetic conductive plate, 7: upper magnetic conductive gasket, 8: GMM rod, 9: coil frame, 10: pickup coil, 11: under magnetic conductive gasket, 12: stainless steel ring, 13: Hall sensor, 14: under magnetic conductive plate, 15: excitation coil, 16: nonmagnetic glue.

nal magnetic circuit interfering from external environment. The disk spring is a preload device which provides a pre-tightening force to the internal core structure of GMM rod, etc. to prevent it from loosening. In order to guarantee the stationary of whole structure and realize fine adjustment of pre-tightening force conveniently, two disk springs with involution combination mode is adopted. The pre-tightening force can be adjusted with the thread fit distance between mounting cover and outer sleeve. In addition, end cover, coil frame, upper and under magnetic conductive plate are interference fit to the outer sleeve to prevent these parts from loosening.

Therefore based on the inverse magnetostrictive effect mechanism and GMM properties, a giant magnetostrictive force sensor which can measure static and dynamic force simultaneously mainly comprises of: GMM generating inverse magnetostrictive effect, DC excitation coil or permanent magnet making GMM rod premagnetization, magnetic flux guiding structure, measuring devices of static and dynamic magnetic flux density, exerting force mechanism, and outer sleeve preventing external interference.

3. Sensor model

The giant magnetostrictive force sensor is operated under a certain bias magnetic field. While external force is applied to GMM rod always being in premagnetization, magnetic flux density in GMM rod changes, and even generates induced voltage in pick up coil under a dynamic force. Therefore, output performance is not only related to the external force, but also the bias magnetic field. Establishing model for the sensor is to obtain the relationship among magnetic flux density, induced voltage and force under a certain magnetic field. In this section, a model describing the hysteresis and the interaction of magnetic field and force for the sensor is established through a combination of Jiles–Atherton model and magnetomechanical effect approach. According to the actual working process, the model is divided into two parts: premagnetization model and formal working model.

3.1. The relationship between magnetization and magnetic field intensity

Before the giant magnetostrictive force sensor working formally, the GMM rod is magnetized by a bias magnetic field to make GMM rod reach the optimal state. The premagnetization model calculates the magnetization under bias magnetic field which is the initial values for the formal working model. Under a bias magnetic field H, the time rate of change of magnetization M is expressed as:

$$\frac{\mathrm{d}M}{\mathrm{d}t} = \frac{\partial M}{\partial H}\frac{\mathrm{d}H}{\mathrm{d}t} \tag{1}$$

The Jiles–Atherton domain wall model is considered here as a basis for characterizing the magnetic field effect $\partial M/\partial H$ [21]. The magnetic field derivative $\mathrm{d}H/\mathrm{d}t$ is determined by the bias magnetic field generated by excitation coil.

The differential susceptibility $\partial M/\partial H$ is established through consideration of the energy lost when GMM rod is exposed to a magnetic field. Under the action of a magnetic field, magnetic moments rotate toward the magnetic field direction, giving rise to the process of domain wall motion and domain magnetization rotation [21]. Magnetic domains rearrange so as to minimize the total energy, thus producing changes in the magnetization [22,23]. Combining with anhysteretic magnetization M_{an} which is calculated using a modified formulation of Langevin equation, the relation model of magnetization and magnetic field intensity is obtained. In this model, total magnetization is composed of reversible magnetization M_{rev} and irreversible magnetization M_{irr}. The material's effective magnetic field H_{eh}, anhysteretic magnetization, irreversible magnetization, reversible magnetization and total magnetization are as follows:

$$H_{\mathrm{eh}} = H + \alpha M \tag{2}$$

where α is the dimension coefficient related to magnetization process.

Anhysteretic magnetization is quantified using Langevin function [21,24].

$$M_{an} = M_s L\frac{H_{eh}}{a} = M_s\left(\coth\left(\frac{H_{eh}}{a}\right) - \frac{a}{H_{eh}}\right) \tag{3}$$

where coefficient a represents the effective domain density.

The irreversible magnetization, its derivative with respect to magnetic field intensity and the reversible component of magnetization can be shown to be [21]

$$M_{irr} = M_{an} - k\delta\frac{\partial M_{irr}}{\partial H_{eh}} \tag{4}$$

$$\frac{\partial M_{irr}}{\partial H} = \frac{\partial M_{irr}}{\partial H_{eh}}\frac{\partial H_{eh}}{\partial H} = \frac{M_{an} - M_{irr}}{\delta k - \alpha(M_{an} - M_{irr})} \tag{5}$$

$$M_{rev} = c_1(M_{an} - M_{irr}) \tag{6}$$

where k is irreversible loss coefficient, parameter δ is +1 when $dH/dt > 0$ and −1 when $dH/dt < 0$, c_1 quantifies the amount by which domain walls bulge before breaking away from pinning sites.

The total magnetization is then dictated by the superposition of the irreversible and reversible magnetization. Correspondingly, the total differential susceptibility is obtained.

$$M = M_{irr} + M_{rev} \tag{7}$$

$$\frac{\partial M}{\partial H} = \frac{\partial M_{irr}}{\partial H} + \frac{\partial M_{rev}}{\partial H} = (1 - c_1)\frac{M_{an} - M_{irr}}{\delta k - \alpha(M_{an} - M_{irr})} + c_1\frac{\partial M_{an}}{\partial H} \tag{8}$$

Substituting Eqs. (6) and (7) into Eq. (8), the irreversible magnetization is eliminated and another expression of the total differential susceptibility is derived:

$$\frac{\partial M}{\partial H} = \frac{(1 - c_1)(M_{an} - M)}{(1 - c_1)\delta k - \alpha(M_{an} - M)} + c_1\frac{\partial M_{an}}{\partial H} \tag{9}$$

3.2. The relationship between magnetization and stress

After the sensor reaching the premagnetization state, it begins to work formally under an external force. The time rate of change of magnetization under external force is expressed as:

$$\frac{dM}{dt} = \frac{\partial M}{\partial \sigma}\frac{d\sigma}{dt} \tag{10}$$

A law of approach to the anhysteretic magnetization and magnetomechanical effect approach are adopted to quantify the magnetomechanical effect $\partial M/\partial\sigma$ [25]. The stress derivative $d\sigma/dt$ is determined by force applying to GMM rod respectively.

Based on the assumption that hysteresis originates primarily from domain wall pinning and the freeing of domain walls from their pinning sites cause the magnetization to change in such a way as to approach the anhysteretic state, Jiles proposed a magnetomechanical effect approach which can describe change in magnetization $\partial M/\partial\sigma$ that a magnetostrictive material undergoes when subjected to a uniaxial stress effectively [25]. In this model, the effective magnetic field $H_{e\sigma}$ related to stress, material's magnetostrictive coefficient λ, anhysteretic magnetization $M_{a\sigma}$ related to stress, and the elastic energy W of magnetic domain movement caused by stress are as follows:

$$H_{e\sigma} = H + \alpha M + \frac{3}{2}\frac{\sigma}{\mu_0}\frac{\partial\lambda}{\partial M} \tag{11}$$

where μ_0 is the permeability of vacuum.

When magnetic field is applied perpendicular to the axis in which the magnetic moments have been aligned by application of sufficiently large compression on polycrystalline material, domain rotation is the prevailing magnetization mechanism. In view of this situation, Dapino proposed the magnetostriction along the field direction in Eq. (12) [26]. It is not sufficiently general while domain wall motion is more significant, such as the compressive stress action on a GMM rod is relatively small. Therefore, the expression is expanded to provide a more general magnetostriction model in Eq. (13).

$$\lambda = \frac{3}{2}\lambda_s\left(\frac{M}{M_s}\right)^2 \tag{12}$$

$$\lambda = \gamma_1 M^2 + \gamma_2 M^4 \tag{13}$$

where λ_s and M_s are saturation magnetostriction and saturation magnetization, γ_1 and γ_2 are second order and fourth order magnetostrictive coefficient respectively.

Substituting Eq. (13) into Eq. (11) yields:

$$H_{e\sigma} = H + \left(\alpha + \frac{\sigma(3\gamma_1 + 6\gamma_2 M^2)}{\mu_0}\right)M = H + \alpha_\sigma M \tag{14}$$

where $\alpha_\sigma = \alpha + (\sigma(3\gamma_1 + 6\gamma_2 M^2)/\mu_0)$.

Anhysteretic magnetization related to stress is quantified using Langevin function [24,25].

$$M_{a\sigma} = M_s L\frac{H_{e\sigma}}{a} = M_s\left(\coth\left(\frac{H_{e\sigma}}{a}\right) - \frac{a}{H_{e\sigma}}\right) \tag{15}$$

The total magnetization is instead of anhysteretic magnetization in Eq. (14) and Eqs. (14) and (15) become:

$$H_{e\sigma} = H + \alpha_a M_{a\sigma} \tag{16}$$

$$M_{a\sigma} = M_s\left(\coth\left(\frac{H + \alpha_a M_{a\sigma}}{a}\right) - \frac{a}{H + \alpha_\sigma M_{a\sigma}}\right) \tag{17}$$

The elastic energy of per unit volume supplied to the GMM rod by the changing applied stress depends on the square of stress [25]:

$$W = \frac{\sigma^2}{2E} \tag{18}$$

where E is the material elastic modulus.

According to magnetomechanical effect, irreversible magnetization and reversible magnetization caused by elastic energy are defined as respectively [25]:

$$\frac{\partial M_{irr}}{\partial W} = \frac{1}{\xi}(M_{a\sigma} - M_{irr}) \tag{19}$$

$$M_{rev} = c_2(M_{a\sigma} - M_{irr}) \tag{20}$$

where ξ is coefficient with dimensions of energy per unit volume, c_2 describes the flexibility of the magnetic domain walls.

Combining Eqs. (19) and (20) with the derivative of elastic energy with respect to stress gained from Eq. (18), the derivative of the irreversible magnetization with respect to stress is obtained:

$$\frac{\partial M_{irr}}{\partial\sigma} = \frac{\partial M_{irr}}{\partial W}\frac{dW}{d\sigma} = \frac{\sigma}{E\xi}(M_{a\sigma} - M_{irr}) = \frac{\sigma}{\varepsilon^2}(M_{a\sigma} - M_{irr}) \tag{21}$$

where $\varepsilon^2 = E\xi$.

The total magnetization is then dictated by the superposition of the irreversible and reversible magnetization, and the derivative of total magnetization with respect to stress is obtained:

$$\frac{\partial M}{\partial\sigma} = \frac{\partial M_{irr}}{\partial\sigma} + \frac{\partial M_{rev}}{\partial\sigma} = \frac{1}{\varepsilon^2}\sigma(1 - c_2)(M_{a\sigma} - M_{irr}) + c_2\frac{\partial M_{a\sigma}}{\partial\sigma} \tag{22}$$

Substituting Eqs. (7) and (20) into Eq. (22), the irreversible magnetization is eliminated and another relation formula between total magnetization and stress is obtained:

$$\frac{\partial M}{\partial\sigma} = \frac{1}{\varepsilon^2}\sigma(M_{a\sigma} - M) + c_2\frac{\partial M_{a\sigma}}{\partial\sigma} \tag{23}$$

3.3. Magnetic flux density and induced voltage

Under an external force, the total magnetization is solved from Eq. (11) to Eq. (23) using the magnetization calculated from premagnetization model composed of Eqs. (1)–(9) as the initial values. It is substituted into Eq. (24), and the magnetic flux density B can be determined.

$$B = \mu_0(M + H) \tag{24}$$

When the sensor is under the action of a dynamic force, the induced voltage in pick up coil can be obtained according to the Faraday electromagnetic induction law.

$$U = -N\frac{d\phi}{dt} = -NA\frac{dB}{dt} = -NA\frac{d[\mu_0(M+H)]}{dt} \tag{25}$$

where A is the cross sectional area of pick up coil.

Substituting the stress ($\sigma = F/A_r$) and the time rate of change of magnetization into Eq. (25), the relation formula between induced voltage and force is derived:

$$U = \frac{-NA\mu_0}{A_r}\left[\frac{(1-c_2)(M_{a\sigma}-M_{irr})F}{\varepsilon^2 A_r} + \frac{c_2\partial M_{a\sigma}}{\partial\sigma}\right]\frac{dF}{dt} \tag{26}$$

where parameters F is the force applied to GMM rod, and A_r is the cross sectional area of GMM rod.

4. Model simulation and experimental validation

4.1. Numerical solution of the model

The working process of the giant magnetostrictive force sensor is divided into two phases. Firstly, DC current is inputted to excitation coil to generate bias magnetic field and the GMM rod reaches a steady premagnetization state. Then, under the premagnetization state, external force is applied directly to the exerting force mechanism and transferred to GMM rod. The sensor works formally. Consequently, the model simulation is carried out in two stages correspondingly and the simulation process is shown in Fig. 2.

Stage 1: There is only the bias magnetic field acting on the sensor and the external force F (stress σ) is 0. The magnetic field intensity increases from 0 to maximum H_{max} gradually. Then it is reduced to H_0 at which the sensor works normally and keeps constant. The concrete calculated process is as follows:

(1) Initialization parameters: the initial values of anhysteretic magnetization M_{an}, irreversible magnetization M_{irr} and total magnetization M are set as 0.
(2) Calculating the anhysteretic magnetization and irreversible magnetization: the anhysteretic magnetization is solved by Eq. (3). The differential Eq. (5) is solved using the improved Euler method and the irreversible magnetization is obtained.
(3) According to Eqs. (6) and (7), the reversible magnetization and total magnetization are derived.

Stage 2: On the basis of magnetic field intensity H_0 being kept constant, external force F is applied to the sensor and the sensor begins to work formally. Correspondingly, the magnetic flux density in GMM rod changes and there is induced voltage in pickup coil. The concrete calculated process is as follows.

(1) Initialization magnetic parameters: the initial values of anhysteretic magnetization $M_{a\sigma}$ and irreversible magnetization M_{irr} are equal to the last group of values M_{an} and M_{irr} respectively in the first stage.
(2) Solving the anhysteretic magnetization, reversible and irreversible magnetization: the Newton iterative method is adopted to solve Eq. (15), and the anhysteretic magnetization and its derivative with respect to stress are obtained. Then, on the basis of solved anhysteretic magnetization, the irreversible and reversible magnetizations are derived from Eqs. (21) and (20), respectively.
(3) Finally, based on Eq. (26), the induced voltage generated in pick up coil under the action of the force is obtained.

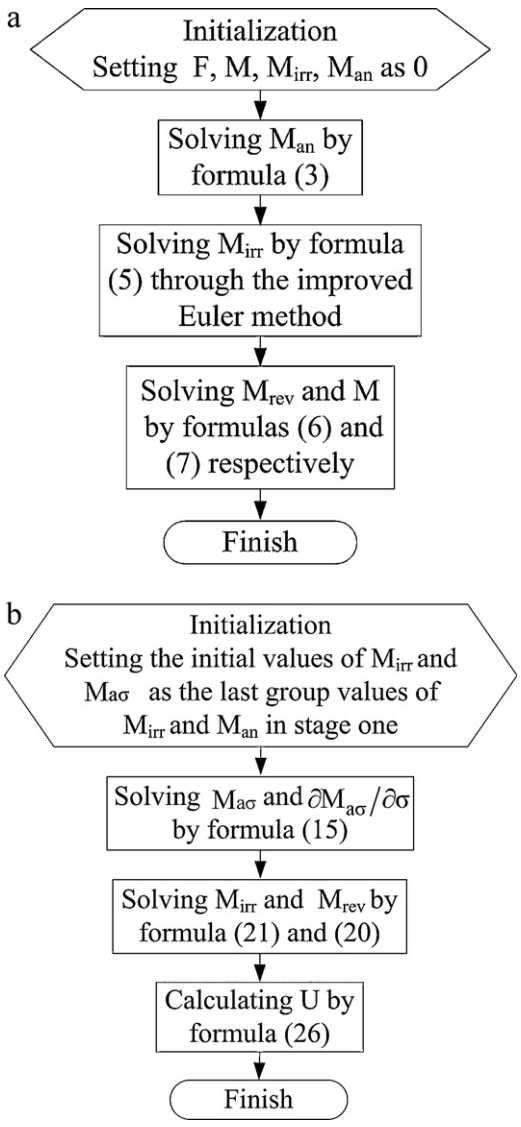

Fig. 2. Numerical solution flowchart: (a) Stage 1 and (b) Stage 2.

4.2. Identification of model parameters

There are nine unknown magnetic and magnetostrictive parameters in the sensor model, that is a, M_s, α, c_1, k_1, γ_1, γ_2, ξ and c_2. These parameters are related to the components and production processes of GMM rod, therefore, it needs to identify these parameters of GMM rod used in the sensor actually. The approach which is a combination of genetic algorithm and simulated annealing algorithm are used to identify these parameters. First, the initial parameter populations are crossed and mutated using the fast search ability of genetic algorithm and a group of optimum parameters are obtained. Then the parameter populations are optimized and adjusted using the sudden jump ability of simulated annealing algorithm. In the identification process, the optimum reserved strategy and dynamic step search method are adopted. It not only makes the algorithm converge faster, but also improves the identi-

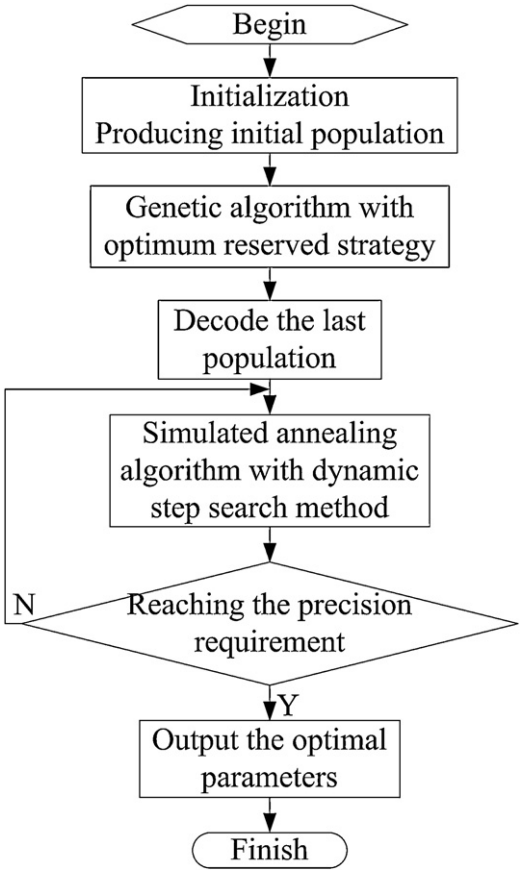

Fig. 3. Parameters identification flowchart.

fication precision and quality of the optimal solution. The concrete process of parameters identification and identification result are shown in Fig. 3 and Table 1.

4.3. Result and discussion

Utilizing the identified magnetic and magnetostrictive parameters in Table 1, the calculated magnetization in first stage and second stage are shown in Fig. 4. In the first stage, magnetic field intensity increases from 0 kA/m to the maximum value 120 kA/m, and subsequently reduces to 10 kA/m under which the sensor works formally. From Fig. 4(a), it can be seen that the final values of M, M_{an}, M_{irr} and M_{rev} are 520.8 kA/m, 401.8 kA/m, 550.5 kA/m, −29.8 kA/m respectively. The final values of M_{irr} and M_{rev} are used as the initial values in the second stage and the calculated result under the action of force is shown in Fig. 4(b). The anhysteretic magnetization $M_{a\sigma}$ is the magnetization in the ideal state where is not mechanical energy loss. Thus, $M_{a\sigma}$ and stress σ present a single value nonlinearity relationship while the magnetic field is constant. $M_{a\sigma}$ increases with increasing σ, it reaches an equilibrium state when σ is at −320 MPa approximately. The irreversible magnetization M_{irr} decreases rapidly with the increasing of σ. However, when σ exceeds −260 MPa, it decreases slowly. When σ is about −300 MPa, M_{irr} reduces to $M_{a\sigma}$ and keeps constant. According to Eq. (20), reversible magnetization M_{rev} is proportional to $M_{a\sigma} - M_{irr}$.

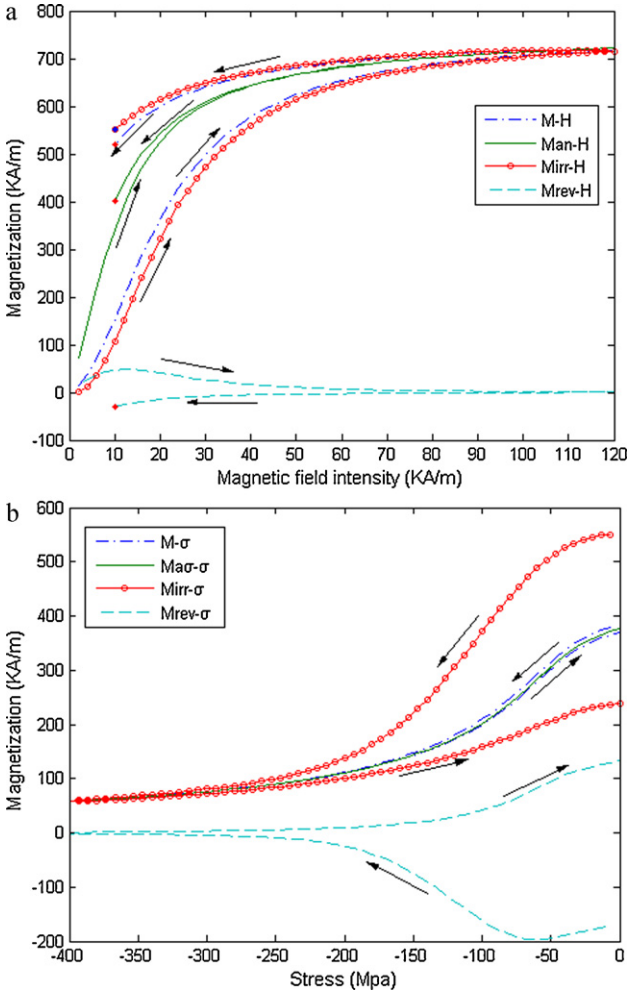

Fig. 4. Magnetization simulation result under magnetic field and stress: (a) magnetization under magnetic field and (b) magnetization under stress.

Therefore, just as shown in Fig. 4(b), when $M_{a\sigma} - M_{irr}$ is increasing, M_{rev} changes rapidly. $M_{a\sigma}$ is equal to M_{irr} and M_{rev} is close to zero when σ is about −350 MPa.

In order to verify the sensor model established in Section 3, a prototype sensor is fabricated to experiment in the experimental system shown in Fig. 5. The GMM rod used in the sensor is TbDyFe with 44 mm length and 12 mm diameter and the pickup coil has 1000 turns. DC current is provided by the bipolar programmable power (BP4610) to excitation coil. The dynamic force applied to the sensor is provided by a vibration exciter and measured by a piezoelectric force sensor. The output induced voltage signal and input force signal are collected and displayed by an oscilloscope.

The experimental results and simulation results are shown in Figs. 6 and 7 respectively. Two groups of sinusoidal force with 10 N amplitude, 500 Hz and 800 Hz frequencies are applied to the giant magnetostrictive force sensor respectively. The sensor works at the bias magnetic fields of 24.5 kA/m and 13 kA/m respectively. It is shown that the induced voltage in pickup coil is harmonic and its frequency is the same as the force. The induced voltages peak–peak are 200 mV and 1.28 V respectively under the two groups of sinu-

Table 1
Parameters identification result.

Parameters	a	M_s	α	c_1	k_1	γ_1	γ_2	ξ	c_2
Value range	$[1,8]\times10^3$	$[1,8]\times10^5$	$[-0.01, 0.01]$	$[0, 0.04]$	$[1,8]\times10^3$	$[0,6]\times10^{-15}$	$[-5,0]\times10^{-29}$	$[5,10]\times10^3$	$[0.2, 1.5]$
Results	7.806×10^3	7.905×10^5	0.007	0.002	1.892×10^3	2.196×10^{-15}	-1.223×10^{-29}	8.792×10^3	0.883

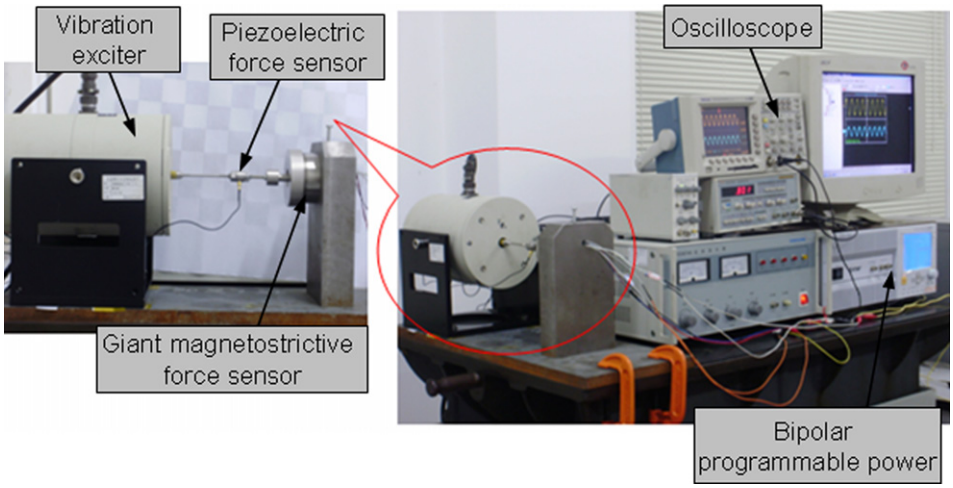

Fig. 5. Experimental system.

soidal force. From the comparison result between the simulation results of the model and the experimental results, it is known that the model provides a very accurate representation of the induced voltage in the giant magnetostrictive force sensor in both the amplitude and frequency of the measured response. Furthermore, there is a $\pi/9$ phase lag of the model approximately which may be caused by eddy current losses in the GMM rod.

5. Sensitivity analysis

In this section, the responses of the giant magnetostrictive force sensor to applied forces are studied through experiment to determine the sensitivity of the sensor. The sensor output signal used in this experiment is the normalized voltage (U_N), which is defined

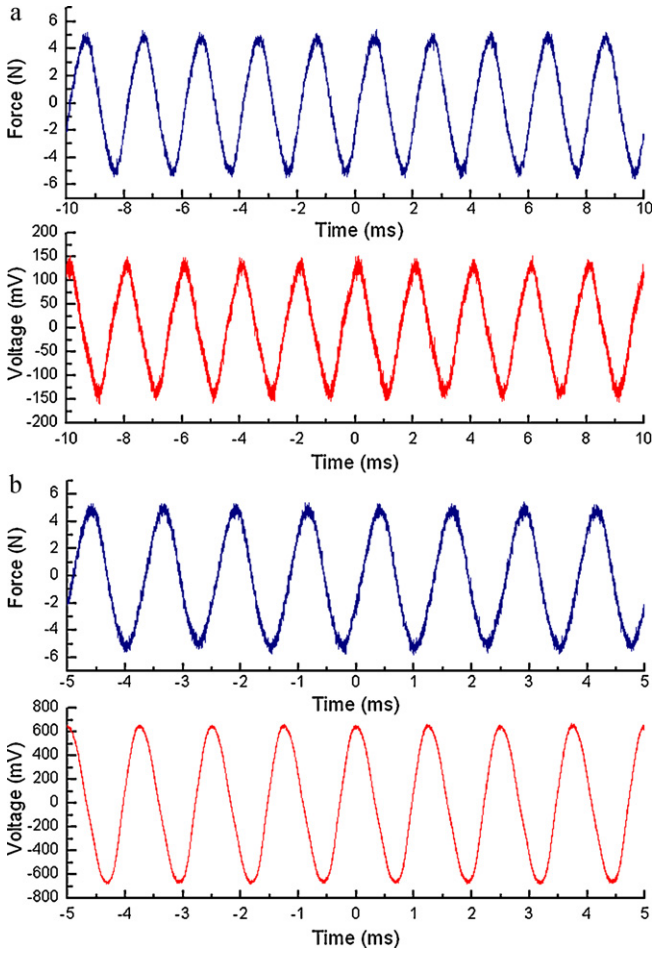

Fig. 6. Experimental results of the sensor: (a) $f = 500$ Hz, $H_0 = 24.5$ kA/m and (b) $f = 800$ Hz, $H_0 = 13$ kA/m.

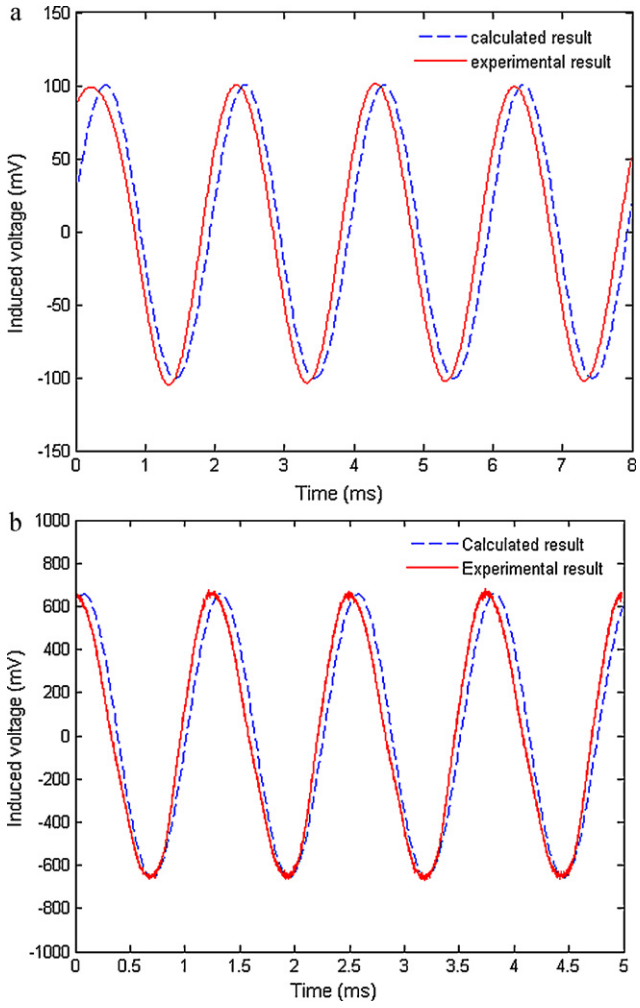

Fig. 7. Comparison of simulation and experimental results: (a) $f = 500$ Hz, $H_0 = 24.5$ kA/m and (b) $f = 800$ Hz, $H_0 = 13$ kA/m.

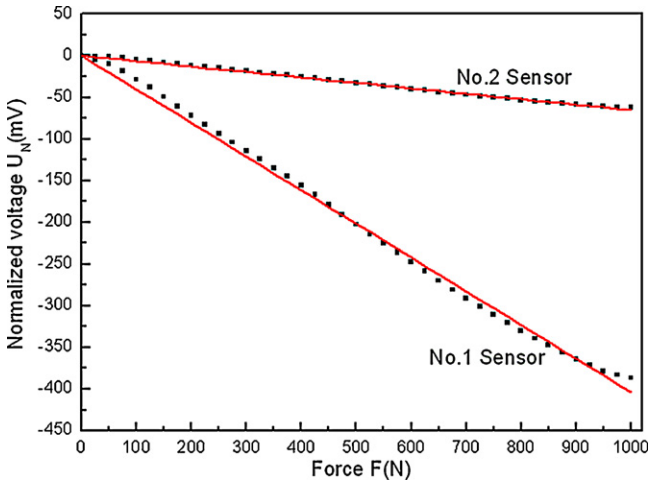

Fig. 8. Output result comparison between No. 1 and No. 2 sensors.

as:

$$U_N = U_H - U_0 \tag{27}$$

In which, U_0 is the output voltage with zero applied force. U_H is the output voltage when the sensor is subjected to a known force. The normalized voltage obviously represents the net change in output voltage when the sensor is subjected to a given force difference. Thus, the force sensitivity of the sensor (S) based on normalized voltage is defined as:

$$S = \frac{\partial U_N}{\partial F} \tag{28}$$

In studying force measuring sensitivity of the sensor, it is carried out experiment under the bias excitation current 3 A. Forces are applied to the sensor from 0 N to 1000 N in 25 N increments. The sensor output voltages are recorded at each force and are normalized according to Eq. (27). The normalized voltages as a function of applied force together with the best-fit straight line are presented in Fig. 8. The slope of the best-fit line to data in Fig. 8 represents the force sensitivity of the giant magnetostrictive force sensor and the sensitivity is about −0.40 mV/N.

In order to evaluate the sensitivity of the sensor designed in the paper (No. 1 sensor), its output is compared to a sensor which does not have the special structure of a stainless steel ring (No. 2 sensor). In this comparison, the same experiment under 3 A bias excitation current is carried out for No. 2 sensor. The normalized voltage from Eq. (27) and its best-fit line are also shown in Fig. 8. The No. 2 sensor is expected to produce approximately −0.065 mV for 1 N force. The No. 1 sensor obviously produces much more output voltage for the same force than the sensor without a stainless steel ring. The giant magnetostrictive force sensor designed in the paper has a 6.14 times higher sensitivity than that of No. 2 sensor approximately. The special structure of a stainless steel ring surrounding the Hall sensor improves the sensitivity obviously.

6. Conclusions

In this paper, according to the analysis of inverse magnetostrictive effect mechanism and GMM properties, a novel giant magnetostrictive force sensor using a GMM rod as the sensitive element is designed. The sensor can measure static and dynamic force simultaneously. It realizes static force and dynamic force measuring through an integrated linear Hall sensor which measures the variation of magnetic flux density in GMM rod and a pickup coil which measures the induced voltage respectively. A special structure around Hall sensor with a stainless steel ring is proposed and the sensitivity is improved. Based on experiment analysis, the sensitivity is about −0.40 mV/N and is 6.14 times higher than that of the sensor without a stainless steel ring. In addition, a model describing the hysteresis and the interaction of magnetic field and force for the sensor designed in the paper is established through a combination of Jiles–Atherton model and magnetomechanical effect approach. The detailed numerical solution process model is presented, and the unknown magnetic and magnetostrictive parameters are identified by a hybrid algorithm of genetic algorithm and simulated annealing algorithm. The simulation results show that the model can reveal the process mechanism of magnetization and has a good ability in describing the hysteretic nonlinearity. The experimental results demonstrate that the model can preferably characterize the output performance of the sensor under a constant magnetic field and external force. It lays a foundation for the further study and accurate control of giant magnetostrictive force sensor. The future work which needs to be done is finding the reason of phase lag and correction model.

Acknowledgements

The work was supported by the National Natural Science Foundation of China under Grant No. 50775021.

References

[1] T.A. Baudendistel, M.L. Turner, IEEE Sens. J. 7 (2007) 245–250.
[2] Q.X. Yang, R.G. Yan, C.Z. Fan, F.G. Liu, S. Liu, IEEE Trans. Magn. 43 (2007) 1437–1440.
[3] O. Geoffroy, D. O'Brien, O. Cugat, J. Delamare, IEEE Trans. Magn. 46 (2010) 666–669.
[4] Z.Y. Jia, X.H. Lu, F.J. Wang, W. Liu, China Mech. Eng. 20 (2009) 1965–1969.
[5] D.K. Kleinke, H.M. Uras, Rev. Sci. Instrum. 65 (1994) 1699–1710.
[6] J.J. Liu, P.Z. Si, W.S. Zhang, X.C. Liu, J. Alloys Compd. 474 (2009) 9–13.
[7] X.K. Lv, S.W. Or, W. Liu, X.H. Liu, Z.D. Zhang, J. Alloys Compd. 476 (2009) 24–27.
[8] A.G. Olabi, A. Grunwald, Mater. Des. 29 (2008) 469–483.
[9] Y.J. Wang, X.Y. Zhao, J. Jiao, L.H. Liu, W.N. Di, H.S. Luo, S.W. Or, J. Alloys Compd. 500 (2010) 224–226.
[10] Y.J. Wang, X.Y. Zhao, J. Jiao, Q.H. Zhang, W.N. Di, H.S. Luo, C.M. Leung, S.W. Or, J. Alloys Compd. 496 (2010) L4–L6.
[11] Z.Y. Jia, H.F. Liu, F.J. Wang, Mechatronics 19 (2009) 1191–1196.
[12] Z.Y. Jia, F.J. Wang, C. Shi, Y.S. Zhang, L.S. Guo, J. Dalian Univ. Technol. 44 (2004) 824–829.
[13] Z.Y. Jia, X.Y. Wang, F.J. Wang, J. Dalian Univ. Technol. 48 (2008) 269–273.
[14] A. Grunwald, A.G. Olabi, Sens. Actuators, A 144 (2008) 161–175.
[15] R. Angara, L. Si, M. Anjanappa, Smart Mater. Struct. 18 (2009) 1–7.
[16] Y.M. Pei, X. Feng, X. Gao, D.N. Fang, J. Alloys Compd. 476 (2009) 556–559.
[17] X.Y. Wang, PhD thesis. Dalian University of Technology, Dalian, People's Republic of China (2007).
[18] H.M. Zhou, Y.H. Zhou, X.J. Zheng, Q. Ye, J. Wei, J. Magn. Magn. Mater. 321 (2009) 281–290.
[19] K. Linnemann, S. Klinkel, W. Wagner, Int. J. Solids Struct. 46 (2009) 1149–1166.
[20] A. Bergqvist, G. Engdahl, IEEE Trans. Magn. 27 (1991) 4796–4798.
[21] D.C. Jiles, D.L. Atherton, J. Magn. Magn. Mater. 61 (1986) 48–60.
[22] D.C. Jiles, J.B. Thoelke, M.K. Devine, IEEE Trans. Magn. 28 (1992) 27–35.
[23] A. Raghunathan, Y. Melikhov, J.E. Snyder, D.C. Jiles, IEEE Trans. Magn. 45 (2009) 3954–3957.
[24] D. Gordon, V. Krishnamurthy, S.H. Chung, Mol. Phys. 106 (2008) 1353–1361.
[25] D.C. Jiles, J. Phys. D: Appl. Phys. 28 (1995) 1537–1546.
[26] M.J. Dapino, R.C. Smith, A.B. Flatau, IEEE Trans. Magn. 36 (2000) 545–556.